Application of Compressed Sensing to 2D and 3D Relaxometry and Related Experiments

Hasan Celik[1], Ariel Hafftka[2], Alexander Cloninger[3], Wojciech Czaja[2], and Richard G. Spencer[1]

[1]*National Institute on Aging, National Institutes of Health, Baltimore, MD, United States,* [2]*Department of Mathematics, University of Maryland, College Park, MD, United States,* [3]*Applied Mathematics Program, Yale University, New Haven, CT, United States*

Introduction: Multi-exponential NMR transverse relaxation signal from tissue, such as brain, cartilage and muscle, has the potential to define the relative weights and decay time constants of underlying exponentially-decaying components, providing insight into macromolecular composition and characteristics [1-3]. Determining these weights and decay constants requires the solution of an inverse Laplace transform (ILT), which is well-known to be ill-conditioned, rendering it highly sensitive to noise and of potentially limited accuracy. We have recently demonstrated markedly improved stability of two-dimensional (2D) relaxometry, in which relaxation components are characterized by both T_1 and T_2, as compared to the conventional 1D relaxometry[4], under certain conditions. However, acquisition time is roughly proportional to the number of rows of data sampled in the indirect dimension, leading to lengthy acquisition times. Recently, Cloninger et. al., developed a compressed sensing (CS) approach to 2D relaxometry which permits acquisition of only a fraction of the natural complete data set [5]. Results were tested and validated through extensive simulations. In the present work, we apply the CS approach of Cloninger et al. to two experimental systems, olive oil and bovine patella articular cartilage. Further, we present an extension of the algorithm from 2D to 3D, with further experimental validation using the olive oil phantom.

Theory: In 2D relaxometry based on longitudinal and transverse relaxation, acquired data is the superposition of signal from a distribution F(T1, T2), which, in the case of discrete components, is the sum of scaled 2D delta functions. In the 3D case, the acquired data represents signal from a 3D distribution F(T1, T2, P) where the third parameter characterizing spin systems is denoted P. Examples of this third parameter could be T_2*, ADC, or magnetization transfer rate k_m. The acquired data matrix M is related to the distribution F by the tensor product equation $M_{vec} = (K_1 \otimes K_2 \otimes K_3) \bullet F_{vec}$, where M_{vec} and F_{vec} denote the lexicographical reordering of M and F into vectors. Geometrically, M is obtained by multiplying the columns of F by K_1, the rows by K_2, and all columns in the z-direction by K_3. The CS approach to this in 2D involves SVD-based compression, matrix completion, and inversion algorithm described in [6]. To extend this approach to 3D we assume that M is sub-sampled only in the x&y directions, with fully sampled data being acquired in the third dimension using, for example, a CPMG experiment where sub-sampling is not of use. We compute the reduced SVD decomposition of each kernel and compress the data M along the z direction: $M_{compressed} = (I \otimes I \otimes U_3^t) \bullet M_{vec}$ where U_3 is the left singular matrix of K_3. After the compression, the number of x&y slices of M is dramatically reduced, e.g., from 1024 to ~10. Matrix completion is then performed based on a fixed point continuation algorithm[7] to generate the missing elements in the the randomly sub-sampled 2D x-y array. In the 3D case, we apply the same matrix completion algorithm to each x-y slice of the 3D array $M_{compressed}$. Finally, the completed 3D array is uncompressed following $M_{completed} = (I \otimes I \otimes U_3) \bullet M_{completed,compressed}$ and the inverse result F was obtained by following the inversion algorithm described in [6] that was expanded to 3D.

Methods & Materials: Experimental data were collected on a 400 MHz Bruker Avance III NMR spectrometer equipped with a Micro2.5 micro-imaging probe and a 5 mm solenoidal coil. One set of 2D data were acquired using a 2D T_1-T_2 relaxometry pulse sequence consisting of an inversion recovery preparation module with variable inversion times followed by a CPMG sequence with acquisition at echo maxima. A second 2D sequence was also implemented, which consisted of two CPMG sequences separated by a variable delay mixing time, during which exchange between sites occurs. 3D data were acquired using a pulse sequence consisting of the same T_1 and T_2 modules as described above, separated by a stimulated echo diffusion encoding sequence. The olive oil sample was studied at 25° C in a spherical tube to minimize susceptibility effects. The T_1-T_2 experiment was conducted using following parameters: echo time TE=2 ms, number of echoes NE=2048, repetition time TR=5s, number of inversions NI=64 with inversion times sampled logarithmically between 50 and 3250 ms. The articular cartilage sample was placed in Fluorinert to minimize susceptibility effects and studied at 4°C. The subchondral bone was positioned perpendicular to the axis of the magnet to maximize the alignment of the collagen fibers in the cartilage deep zone with B_0. The T_2-exchange-T_2 dataset was acquired using the following parameters: mixing time τ_m =10ms, TE=400μs, TR=8s. Both T_2 dimensions were sampled on a square grid, with a data size of 88x88 after logarithmic decimation of data points. The 3D experiments with olive oil were performed under the same conditions as above, and with the same parameters for the T_1 and T_2 modules. The diffusion sensitization was performed with 64 b-values log-spaced between 1.25 and 5085 s/mm^2, with a diffusion encoding period of Δ=20ms and bipolar encoding gradient duration δ=2 ms for each gradient value.

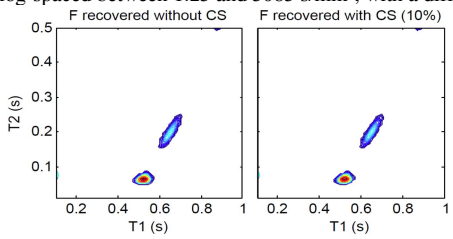

Figure 1. T_1-T_2 histograms for the olive oil sample.

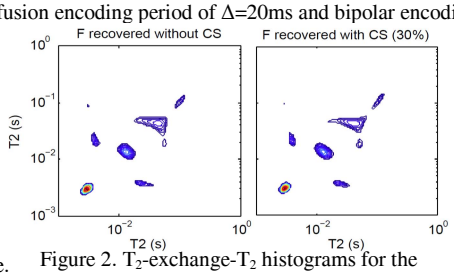

Figure 2. T_2-exchange-T_2 histograms for the bovine articular cartilage sample.

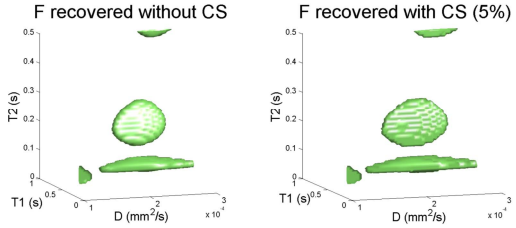

Figure 3. T_1-D-T_2 histograms for the olive oil sample.

Results & Discussion: The 2D T_1-T_2histograms for the olive oil sample are shown in Fig. 1, the 2D T_2-exchange-T_2 histograms for the bovine articular cartilage in Fig. 2 and the 3D T_1-D-T_2 histograms for the olive oil sample in Fig.3. In each figure, results obtained with the full data set (left panel) are compared to results obtained using CS (right panel). Note that the degree of sub-sampling is indicated in the figure heading. Sub-sampling was performed in both dimensions for the 2D comparisons as described by Cloninger in [5], and in the indirect T_1- and D-dimensions for the 3D comparison. The results for the inverse problem with and without CS in Figs. 1 show that the 2D CS algorithm can reduce the data acquisition time by a factor of 10, while maintaining the quality of the results. The T_2-exchange-T_2 data from the bovine articular cartilage poses a more challenging inversion problem due to the presence of off-diagonal peaks, which are absent from the T_1-T_2 data from the olive oil sample. Accordingly less sub-sampling, that is retention of a larger percentage of data points, is necessary to maintain accuracy, resulting in a reduction of acquisition time by a factor of ~3.3. In Fig. 3, the comparison of the left and right panels shows that the 3D CS algorithm can provide accurate results while sub-sampling as low as 5% of the data, speeding up the acquisition time by a factor of 20. The peaks at the edges of the 3D histograms in Fig. 3 are resulting from numerical inaccuracies and ill-conditioned nature of the inversion problem. We note that subsampling in the T_2 direct dimension does not provide any data acquisition advantage, but serves as a model for experiments in which data acquisition is time-consuming in both dimensions.

Conclusion: Use of CS can significantly decrease acquisition times for multidimensional NMR relaxometry and related experiments. Extension of existing 2D results to 3D has been demonstrated, and has the potential to permit these higher-dimensional experiments to be performed in realistic acquisition times. These higher-dimensional experiments have the potential to provide a much more complete characterization of tissue.

References: [1] Mackay, A., et al., *MRM*, 1994. 31(6): p. 673-677. [2] Reiter, D.A., et al.,*MRM*. 65(2): p. 377-384. [3] Saab, G., et al., *MRM*, 2001. 46(6): p. 1093-1098. [4] Celik, H., et al., *JMR*. 236: p. 134-139. [5] Cloninger, A., et al., *SIIMS*. 7(3): p. 1775-1798. [6] Hurliman, L., et.al., *IEEE Trans. Image Process.*, 2002. 50(5): p. 1017-1026. [7] Ma, S., et. al., *Math. Prog.*. 128(1-2): p. 321-353.